

Reliable Force Predictions for a Flapping-wing Micro Air Vehicle: A “Vortex-lift” Approach

W. Thielicke, A.B. Kesel and E.J. Stamhuis

Reprinted from

International Journal of Micro Air Vehicles

Volume 3 · Number 4 · December 2011



Multi-Science Publishing
ISSN 1756-8293

Reliable Force Predictions for a Flapping-wing Micro Air Vehicle: A “Vortex-lift” Approach

W. Thielicke^{a,b}, A.B. Kesel^a and E.J. Stamhuis^b

^aBiomimetics-Innovation-Centre, University of Applied Sciences Bremen, Germany

^bOcean Ecosystems, University of Groningen, The Netherlands

ABSTRACT

Vertical and horizontal force of a flapping-wing micro air vehicle (MAV) has been measured in slow-speed forward flight using a force balance. Detailed information on kinematics was used to estimate forces using a blade-element analysis. Input variables for this analysis are lift and drag coefficients. These coefficients are usually derived from steady-state measurements of a wing in translational flow. Previous studies on insect flight have shown that this method underestimates forces in flapping flight, mainly because it cannot account for additional lift created by unsteady phenomena. We therefore derived lift and drag coefficients using a concept for delta-wings with stably attached leading-edge vortices. Resulting lift coefficients appeared to be a factor of 2.5 higher than steady-flow coefficients, and match the results from previous (numerical) studies on instantaneous lift coefficients in flapping flight. The present study confirms that a blade-element analysis using force coefficients derived from steady-state wind tunnel measurements underestimates vertical force by a factor of approximately two. The equivalent analysis, using “vortex-lift” enhanced coefficients from a delta-wing analogue, yields very good agreement with force balance measurements, and hence seems to be a good approximation for lift-enhancing flow phenomena when modelling flapping flight.

1. INTRODUCTION

The desire to understand the aerodynamics of flapping flight in insects, birds and bats has been the motivation of many studies in the past. Early attempts applied the blade-element theory (BET), a theory often used to estimate thrust and torque of revolving propellers, to explain forces required during sustained insect hovering flight [1]. The basis of this theory is a “quasi-steady” approach that assumes the instantaneous forces of a flapping wing to be identical to the forces of the same wing under steady motion with identical angle of attack and velocity [1]. The idea of the BET is to divide the wings into small elements along the wing span. For each element, the effective angle of attack as well as the instantaneous flow velocity is derived from detailed time-resolved information on the kinematics of the flapping wing. The forces created by each element can be calculated when lift and drag coefficients of the wing sections are known. Usually, these coefficients are derived from static force measurements of a series of angles of attack of the airfoils under steady-flow conditions in a wind tunnel. However, the application of the BET appeared to seriously underestimate the forces observed in flapping insect flight [1–3]. By studying the flow around flapping robotic insect wings, Ellington et al. [4] identified an explanation for this discrepancy. In a scaled model of a hovering hawkmoth, they observed large vortices on top of the wings increasing the circulation and therefore the aerodynamic forces. These leading-edge vortices (LEVs) remain stably attached to the wing and contribute substantially to lift throughout the full downstroke by increasing the amount of bound circulation of the wing. Subsequent studies identified LEVs in other insects, robotic flapping-wing devices, hovering birds and slow-flying bats (e.g. [5–9]). Lentink and Dickinson [10] suggest that LEVs are a universal and efficient high lift mechanism for slow flapping flight over a quite large range of animal sizes. The amplifying effect of these vortices on the lift and drag coefficients during wing flapping [6] is not present when determining lift coefficient (C_L) and drag coefficient (C_D) from steady-flow force measurements in a wind tunnel. Hence, forces calculated with a

blade-element analysis underestimate forces of flapping wings. Although the discovery of LEVs in insect flight substantially contributed to understanding the mechanics of flapping flight, these vortices were well known to aircraft designers before they were found in nature: During relatively slow flight, delta-wing aircrafts like the Concorde largely rely on lift created by additional circulation of stable leading-edge vortices (e.g. [11]). The sharp leading edges of the wings of such aircrafts induce flow separation, a feature that can also be found on insect and bird wings (e.g. [12]). In delta-wing aircrafts, vortices are stabilized by the wing sweep which allows for a spanwise flow parallel to the swept leading edge, convecting vorticity to the wing tip and preventing the LEV to grow and detach [13]. Although the stabilization mechanisms for the LEVs in delta-wing aircraft and flapping insect wings are probably not exactly the same (e.g. [10, 14]), the flow phenomena and the aerodynamic effects of these vortices are analogous [4]. Lift coefficients for delta wings with attached vortical flow on top of the wing range from 4 to 6 [13], which is substantially higher than the lift coefficients of conventional wings.

Polhamus [11] introduces a concept to predict lift coefficients of sharp-edge delta wings (up to an aspect ratio of 4) based on the combination of potential-flow lift and vortex lift. His theory includes a simple trigonometric relationship between the lift (respectively drag) coefficient and geometric angle of attack. The concept was verified by wind-tunnel measurements of sharp-edge, highly swept wings and provides a very good prediction of total lift [15] which may find wider application than for swept wings only.

In the present study, we measured lift and drag of a simple flapping-wing MAV. The MAV is equipped with bio-inspired wings which have a sharp leading edge at the outer $2/3$ of the wing and a round leading edge close to the wing base. Three-dimensional flow patterns around the same type of wing during flapping were analyzed in an earlier study, showing a prominent and stable leading-edge vortex that developed immediately at the beginning of the downstroke [16]. Classical lift and drag coefficients of this type of wing are obtained from steady-flow measurements in a wind tunnel. We use a blade-element analysis to estimate aerodynamic forces, by generating a set of force coefficients using the trigonometric relationship proposed for delta-wings [11] to account for the additional circulation enabled by LEVs. The results of the blade-element analysis using steady-flow force coefficients and force coefficients from a delta-wing analogue are compared to aerodynamic force measurements at the MAV.

2. MATERIALS AND METHODS

2.1. MAV

The wings of the MAV (see Figure 1) are modelled from 3 mm closed-cell extruded polystyrene foam sheet (DEPRON®). The planform is inspired by the wings of swiftlets (*Collocalia linchi*) with some camber at the base and a sharp leading edge at the outer part of the wing. The total wing span (tip-to-tip)



Figure 1: Flapping-wing MAV mounted on the force balance. Wing-span = 0.33 m, average chord length = 40 mm, aspect ratio = 8.3.

is 0.33 m with an average chord length of 40 mm and an aspect ratio of 8.3. The wings are mostly rigid showing only some aeroelastic bending near the tip at higher flapping frequencies, similar to the wings of swifts and swiftlets [16–18].

The wings each have two rotational degrees of freedom (shoulder joint: up and down wing excursion; and longitudinal joint: pro- / supination parallel to the spanwise axis, allowing the wings to change geometric angle of attack (α_{geo} , see Figure 5) and are driven by a single small geared DC motor. Flapping frequency (0–9.5 Hz) was set by altering the voltage of a power supply. The specific arrangement of linkage elements makes the wings supinate during upstroke and pronate during downstroke, resulting in very similar kinematics as in an earlier study that focused on flow measurements [16]. The change of geometric angle of attack and excursion throughout wing beat cycle is shown exemplarily for two different situations in Figure 2.

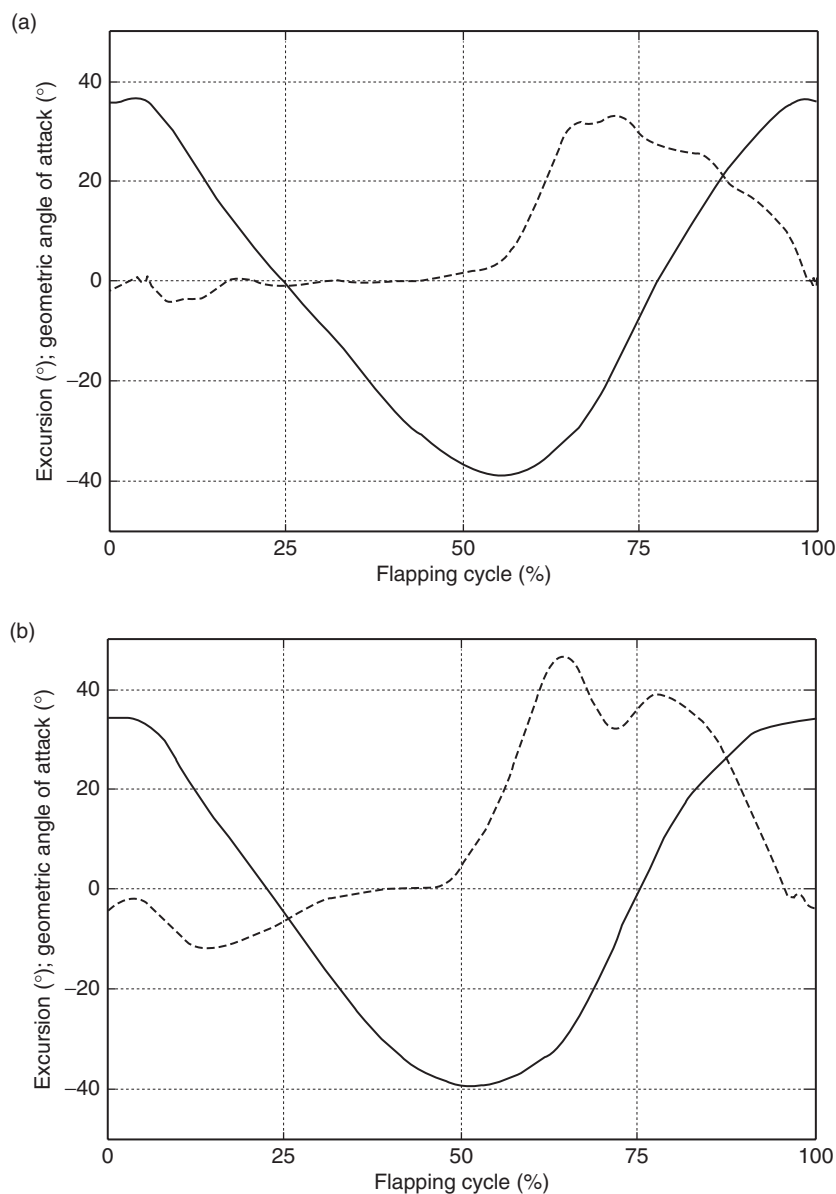


Figure 2: Wing excursion (solid line) and geometric angle of attack (angle between U_f and wing chord; dashed line). (a) Wing kinematics for a flapping frequency of 3.65 Hz in 2.28 m/s flow. (b) Wing kinematics for a flapping frequency of 7.61 Hz in 2.84 m/s flow. The kinematics change at increasing flapping frequency and free flow velocity due to increasing aerodynamic and inertial load and some elasticity in the mechanical design.

The stroke plane was set to 90° in relation to the free flow. To mimic slow-flight conditions, flow velocities between 2.28 m/s and 2.84 m/s were tested in an open jet low speed wind tunnel (test section diameter = 0.45 m; $u_{\max} = 14$ m/s). The Reynolds number (Re), a measure for the importance of inertial vs. viscous forces, is calculated as

$$Re = \sqrt{\frac{\bar{v}_{ip}^2 + U_f^2 * \bar{c}}{\nu}}, \quad (1)$$

where \bar{v}_{ip} = mean vertical tip velocity; U_f = free flow velocity; \bar{c} = mean chord; ν = kinematic viscosity.

Measurements were done for Re between $8*10^3$ and $1.3*10^4$. The advance ratio J , given by

$$J = \frac{U_f}{|\bar{v}_{ip}|} \quad (2)$$

is a measure for forward flight speed vs. wing tip velocity in flapping flight. It ranges from 0.6 to 1.7 for the parameters tested in flapping flight, here.

2.2. Flapping Flight Force Measurements

Vertical (F_V , "lift") and horizontal (F_H , "thrust") force of the MAV was recorded with a 2-axes force balance (for details see [19]), sampled at 1200 Hz, digitized with an analogue-to-digital converter and processed with MATLAB and Excel. Instantaneous forces of eighteen successive full flapping cycles were recorded three times ($n = 3$) for each setup. Flapping frequencies between 3.5 and 9.5 Hz were tested for three flow velocities (2.28; 2.57; 2.84 m/s). Forces were integrated over the wing beat cycle to derive mean horizontal ($\overline{F_H}$) (and mean vertical force ($\overline{F_V}$). The mean vertical force coefficient is derived by

$$\overline{C_V} = \frac{2\overline{F_V}}{\rho U_f^2 A}, \quad (3)$$

where ρ = density; A = total wing area [20].

2.3. Lift and Drag Coefficients

Steady-state lift and drag coefficients (subsequently denominated "steady" coefficients) were obtained from measurements of lift and drag of the isolated wings in the same wind tunnel ($Re = 1.4*10^4$). Forces were sampled for geometric angles of attack between -45° and 65° (step size 1°, $n = 3$). C_L and C_D were derived via

$$C_L = \frac{2F_L}{\rho U_f^2 A}; \text{ respectively } C_D = \frac{2F_D}{\rho U_f^2 A}, \quad (4)$$

where F_L = lift; F_D = drag.

Maximum lift coefficient $C_{L,\max}$ is 1.01 ± 0.01 at 11° geometric angle of attack (see Figure 3). For the blade-element analysis, coefficients were stored in a lookup table, non-integer values were determined via linear interpolation.

An additional set of lift and drag coefficients was created following [11] as explained in short earlier in this paper (subsequently denominated "vortex-lift" coefficients). For a delta-wing with stable leading-edge vortices, total lift coefficient can be approximated using

$$C_L = K_p \sin \alpha \cos^2 \alpha + K_v \cos \alpha \sin^2 \alpha * \frac{\alpha}{|\alpha|} + C_{L_0}, \quad (5)$$

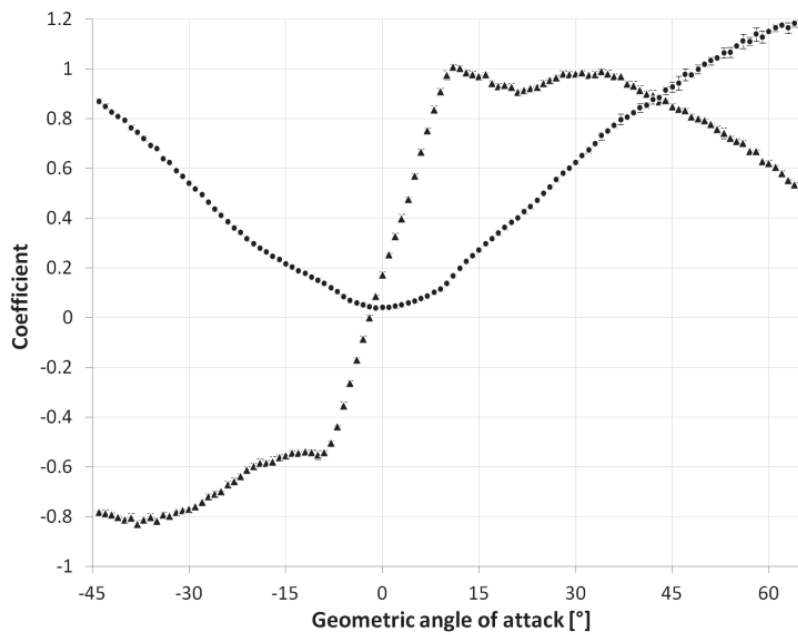


Figure 3: “Steady coefficients”. Lift (triangles) and drag (circles) coefficient of the wings in steady-flow for geometric angles of attack between -45° and 65° ($Re = 1.4 \cdot 10^4$, step size = 1° , $n = 3$).

where α = angle of attack; K_p = constant of proportionality in potential-flow lift term; K_v = constant of proportionality in vortex lift term; C_{L_0} = lift coefficient of the MAV wings at 0° geometric angle of attack.

Polhamus [11] calculated K_p and K_v for aspect ratios up to 4 using a modified Multhopp lifting-surface theory ($K_p = 3.35$; $K_v = 3.45$). Drag coefficient due to lift is given as

$$\Delta C_D = C_L \tan \alpha \quad [15] \tag{6}$$

Total drag coefficient can be approximated as

$$C_D = \Delta C_D + C_{D_0}, \tag{7}$$

where C_{D_0} = drag coefficient of the MAV wings at 0° geometric angle of attack.

Lift and drag coefficients derived with Equation 5 and 7 are plotted in Figure 4.

2.4. Blade-element Analysis

We used a blade-element analysis to predict $\overline{F_V}$ of the flapping-wing MAV using data derived from the wing kinematics and the two different sets of force coefficients (“steady” and “vortex-lift” coefficients). The wing planform was digitized and divided into 496 elements in span wise direction. Lift L_r and drag D_r of each element at distance r from the wing base (see Figure 5 for nomenclature) is calculated using the equation

$$L_r(t) = \frac{1}{2} \rho v_r(t)^2 A_r C_L(\alpha_{eff}), \tag{8}$$

where v_r = effective velocity at r ; A_r = area of wing element r ; α_{eff} = effective angle of attack and

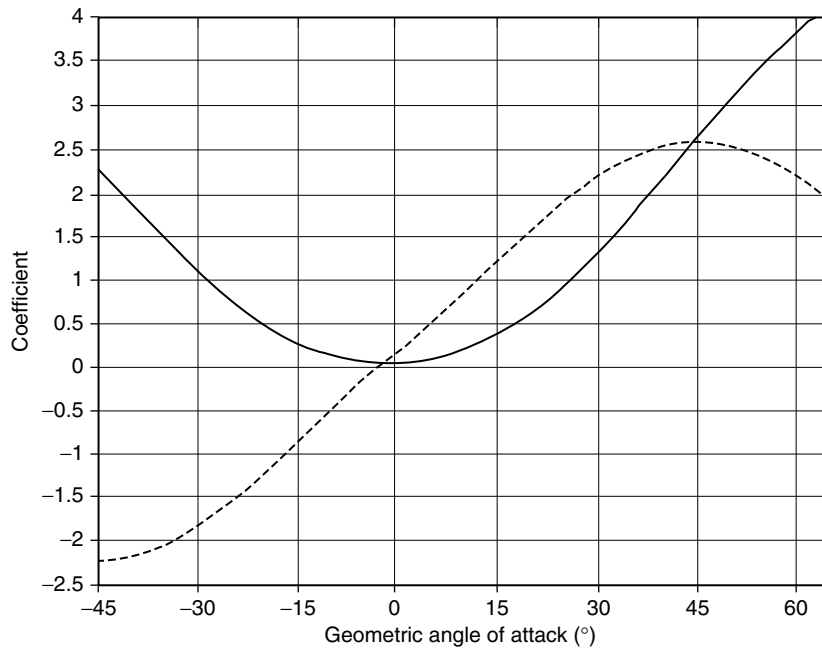


Figure 4: "Vortex-lift" coefficients. Lift (dashed line) and drag (solid line) coefficients for a wing with attached LEVs for geometric angles of attack between -45° and 65° .

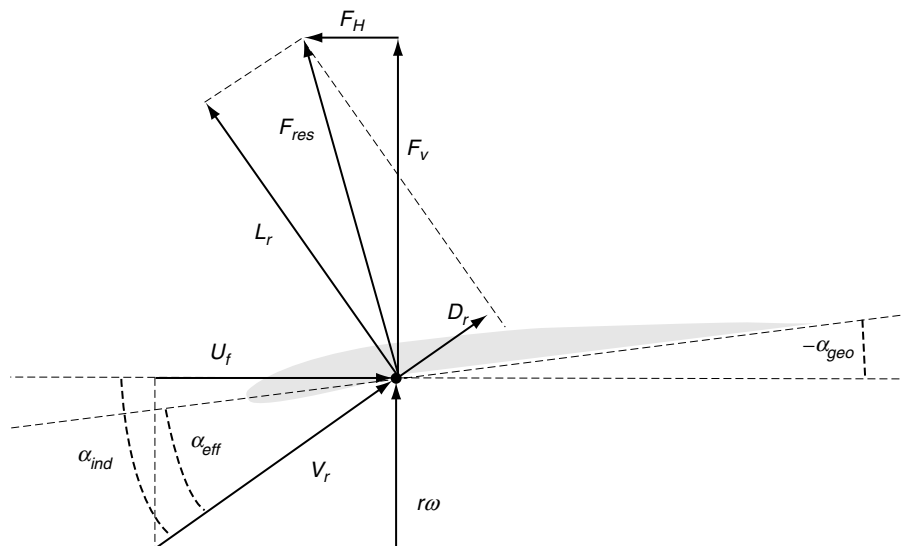


Figure 5: Forces and velocities on a blade-element: α_{eff} = effective angle of attack; α_{geo} = geometric angle of attack; α_{ind} = induced angle of attack; U_f = free flow velocity; v_r = effective velocity; r = radial distance of wing element; ω = angular velocity of the wing; L_r = lift; D_r = drag; F_{res} = resulting force; F_H = horizontal force component; F_V = vertical force component.

$$D_r(t) = \frac{1}{2} \rho v_r(t)^2 A_r C_D(\alpha_{eff}) \tag{9}$$

Effective velocity was calculated as

$$v_r(t) = \sqrt{(r\omega(t))^2 + U_f^2}, \quad (10)$$

where r = radial distance of the wing element to the base; ω = angular velocity (derived from kinematics).

C_L and C_D depend on the effective angle of attack (α_{eff}) of the blade element which is calculated following

$$\alpha_{eff,r}(t) = \alpha_{geo}(t) - \alpha_{ind}(t), \quad (11)$$

where α_{geo} = geometric angle of attack (derived from kinematics); α_{ind} = induced angle of attack = $\text{atan}\left(\frac{r\omega(t)}{U_f}\right)$.

L_r and D_r were integrated for all wing elements and resolved into horizontal (F_H) and vertical (F_V) force components:

$$F_V(t) = \cos(\alpha_{ind}) * L_r(t) + \sin(\alpha_{ind}) * D_r(t) \quad (12)$$

$$F_H(t) = \sin(\alpha_{ind}) * L_r(t) - \cos(\alpha_{ind}) * D_r(t) \quad (13)$$

As the stroke plane of the MAV was set to 90° with respect to U_f , the component of F_V supporting the weight of the MAV changes with angular position of the wing only. Close to the upper or lower turning point of the wings, F_V contributes less than when wings are at mid-down or mid-upstroke. This is accounted for using

$$F_{V,net}(t) = \cos(\Theta(t)) * F_V, \quad (14)$$

where Θ = excursion angle of the wing.

Integrating instantaneous forces over one wing beat cycle for two wings yields mean vertical force ($\overline{F_V}$) and mean horizontal force ($\overline{F_H}$) for two sets of force coefficients, and is compared with the results from mean force measurements at the MAV.

3. RESULTS

3.1. Flapping-wing MAV Force Measurements

In flapping flight, the MAV creates a force perpendicular to U_f (F_V , “lift”) and a force parallel to U_f (F_H , “thrust”). Mean vertical force ($\overline{F_V}$) and mean horizontal force ($\overline{F_H}$) both increase with flapping frequency (Figure 6). $\overline{F_V}$ is always positive for the setups that were tested; increasing U_f also increases maximal $\overline{F_V}$ measured (see Figure 6A). The mean horizontal force is a measure for net thrust. $\overline{F_H}$ is generally lower for high free flow velocities due to increased drag of the whole MAV system, but flapping frequencies > 8 Hz result in net thrust for all flow velocities under test (see Figure 6B). The mean vertical force coefficient increases substantially with decreasing advance ratio compared to the maximum steady-flow lift coefficient ($C_{L,max} = 1.01 \pm 0.01$, $n = 3$) for all but two measurements (see Figure 7).

3.2. Blade-element Analysis

Mean vertical force derived from the blade-element analysis using “steady” C_L and C_D reveals a large defect in force (see Figure 8A-C and summarizing Figure 11). For flapping frequencies above 6 Hz, $\overline{F_V}$ is underestimated by the blade-element approach by a factor of about two. The defect is found in all free flow velocities. The slope of $\overline{F_V}$ vs. frequency calculated via “steady” coefficients is very small, increasing flapping frequencies hardly produce additional $\overline{F_V}$. The defect is smaller for flapping frequencies < 6 Hz (see Figure 8A-C). In contrast, the results of the blade-element analysis using “vortex-lift” coefficients are very similar to experimental results (see Figure 8A-C and Figure 11).

The maximal difference between $\overline{F_V}$ calculated with “vortex-lift” coefficients and the experimental data is 13% (see Figure 9), excluding the data of the two lowest flapping frequencies, which was recorded very close to the resonant frequency of the balance system and is therefore probably not

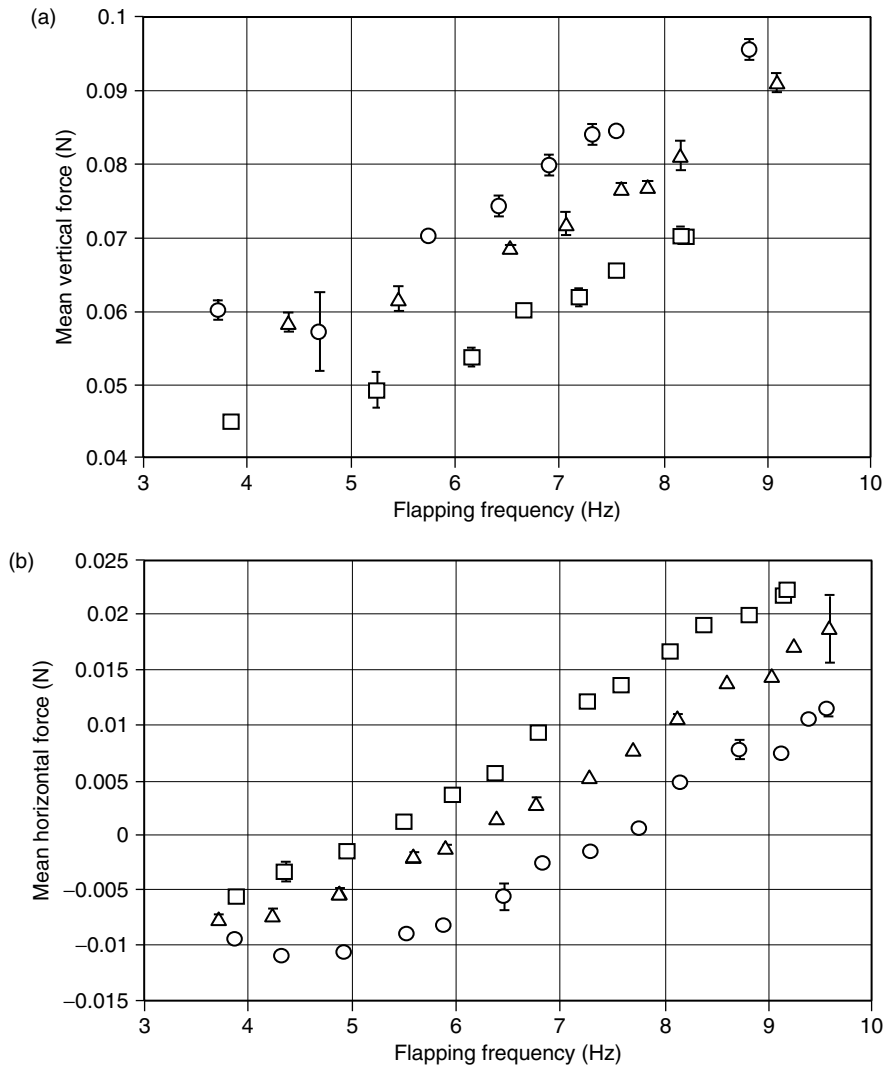


Figure 6: Mean forces of the flapping wings for different U_f ($n = 3$; squares = 2.28 m/s ; triangles = 2.57 m/s ; circles = 2.84 m/s). (a) Mean vertical force (\bar{F}_V) increases with flapping frequency. (b) Mean horizontal force (\bar{F}_H) increases with flapping frequency and becomes positive for high flapping frequencies. Here, the MAV creates "net thrust"

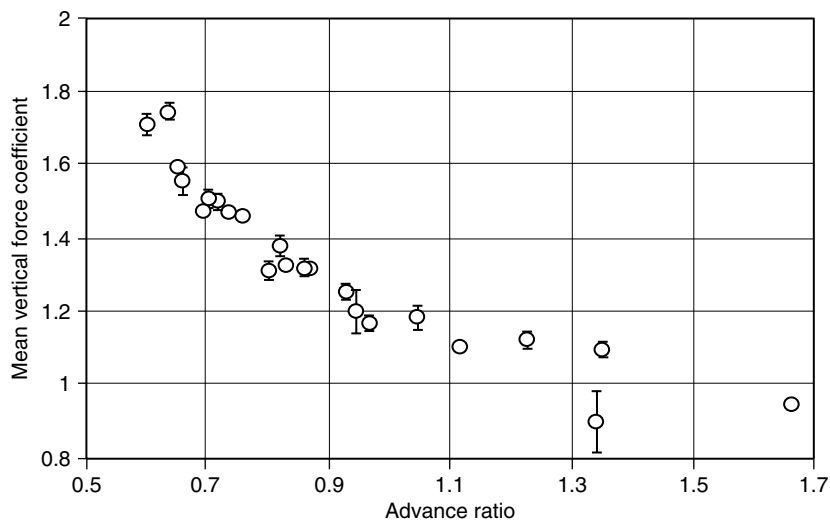


Figure 7: Mean vertical force coefficient (\bar{C}_V) vs. advance ratio. \bar{C}_V peaks at about 1.74 for low advance ratio.

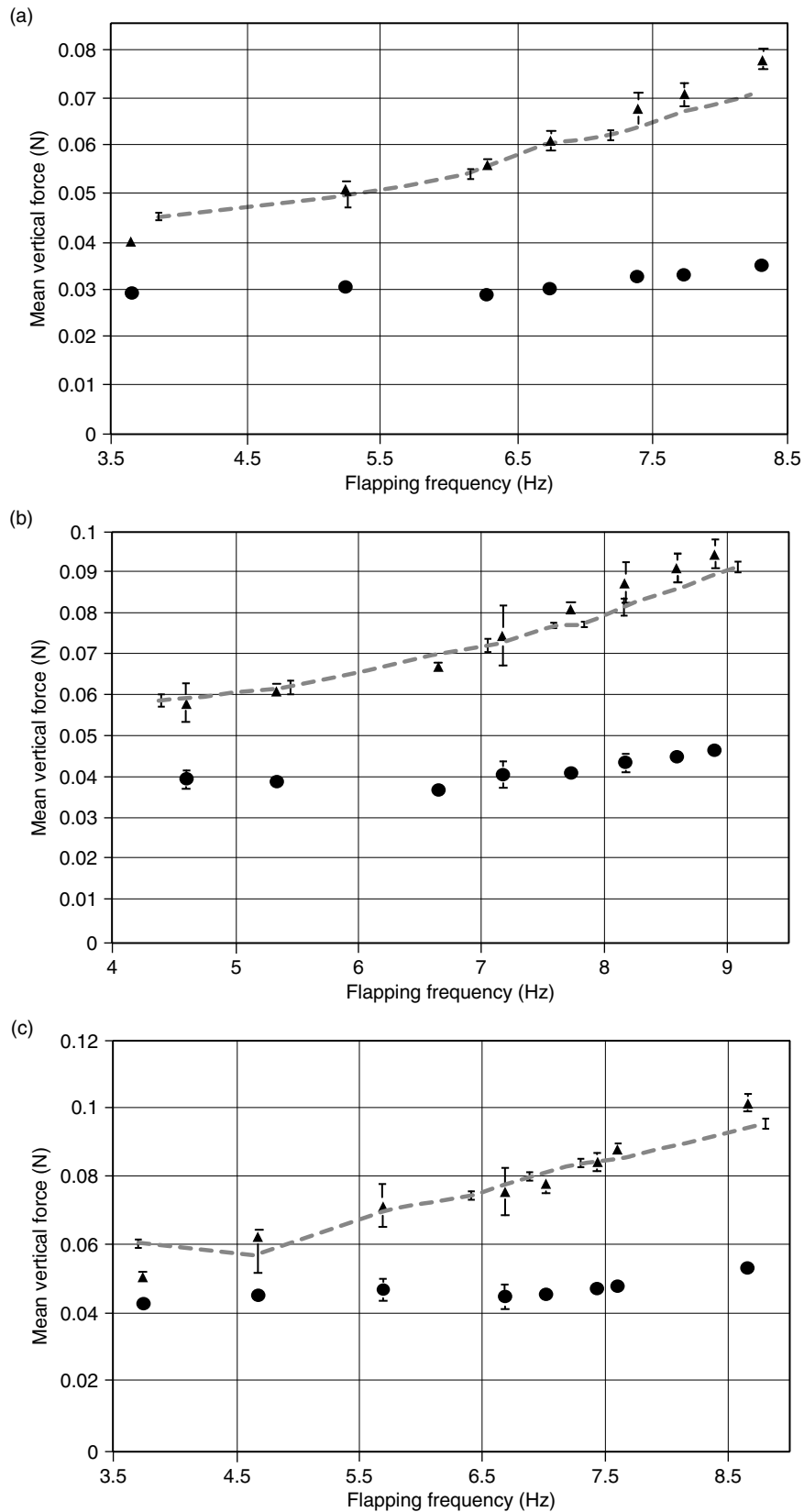


Figure 8: Results of \overline{F}_V for of the blade-element analysis with “steady” (circles) and “vortex-lift” (triangles) force coefficients compared to force balance measurements (dashed line). (a) $U_f = 2.28$ m/s, (b) $U_f = 2.57$ m/s, (c) $U_f = 2.84$ m/s. In all cases, “steady” coefficients underestimate mean vertical force, whereas “vortex-lift” coefficients show a good agreement.

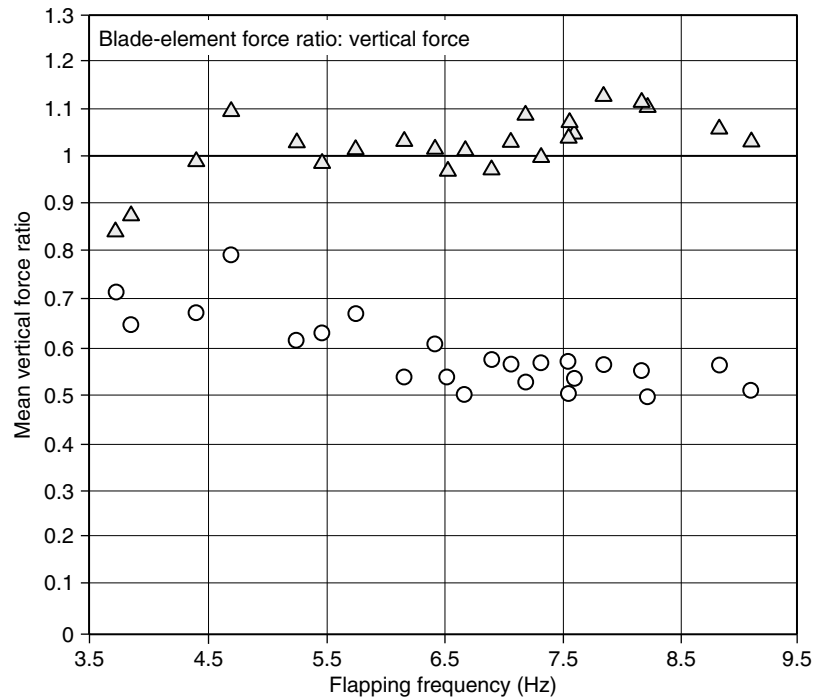


Figure 9: Force ratio: \overline{F}_V (blade-element analysis) divided by \overline{F}_V (experiment). Data for different free flow velocities was pooled. Circles: "Steady" coefficients underestimate \overline{F}_V by a factor of up to two. Triangles: "Vortex-lift" coefficients deviate by maximally 13% (excluding measurements at frequencies close to the resonant frequency of the balance system), and on average by $2.9\% \pm 6.9\%$ ($n = 23$).

reliable. The mean difference in \overline{F}_V of "vortex-lift" coefficients is $2.9\% \pm 6.9\%$; "steady" coefficients result in a mean difference of $-41.6\% \pm 7.5\%$ ($n = 23$).

The blade-element analysis using "vortex-lift" coefficients gives a good estimate for the mean horizontal force (\overline{F}_H , see example in Figure 10A). At increasing flapping frequencies respectively increasing U_f , the match between blade-element analyses and experimental results is less precise (see Figure 10B respectively Figure 11) but the deviation stays proportionally constant. The mean horizontal force predicted by "vortex-lift" coefficients is higher than \overline{F}_H determined with the force balance measurements under these circumstances.

At high flapping frequencies, the blade-element analysis using "steady" coefficients results in an underestimation of \overline{F}_H (see Figure 10B). This underestimation is most apparent for low free flow velocities (see Figure 11).

In all cases, "steady" coefficients underestimate mean vertical force, whereas "vortex-lift" coefficients show a good agreement.

4. DISCUSSION

4.1. Micro Air Vehicle

Vertical and horizontal force of a flapping-wing MAV was determined by means of a force balance. The wings create on average enough vertical and horizontal force to keep a small, fully equipped MAV airborne. Mean vertical force coefficient is inversely related to advance ratio. This is due to the fact that advance ratio decreases with increasing flapping frequency. The increase in flapping frequency causes an increase in the flow velocity over the wing and at the same time increases the effective angle of attack. These all contribute to an increase in aerodynamic force. The relation between mean vertical force coefficient and advance ratio as well as the magnitude of \overline{C}_V is very similar to the results reported by Kim et al. [20]. That study evaluated lift forces of a flapping wing MAV of a size similar to ours but with flexible foil wings, where airfoil camber could be changed using macro-fibre composite actuators. The performance of our MAV design in generating vertical force thus seems to be reliable.

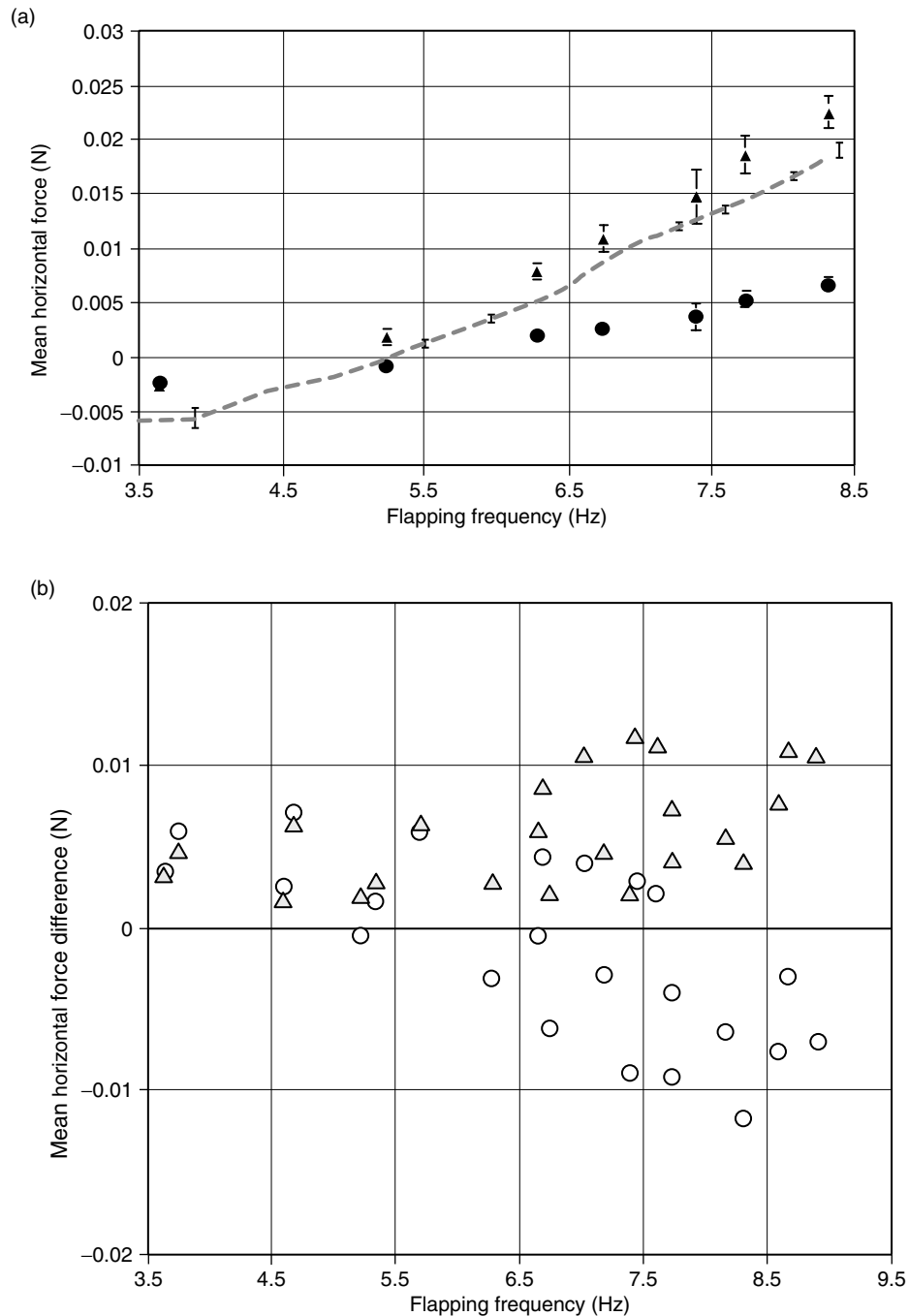


Figure 10: (a) Exemplary result for \overline{F}_H of the blade-element analysis at $U_f = 2.28$ m/s with “steady” (circles) and “vortex-lift” (triangles) force coefficients compared to force balance measurements (dashed line). (b) Force difference of \overline{F}_H (blade-element analysis) minus \overline{F}_H (experiment) for “steady” force coefficients (circles) and “vortex-lift” force coefficients (triangles). Data for different free flow velocities was pooled. At increasing flapping frequencies, “vortex-lift” coefficients tend to overestimate \overline{F}_H , whereas “steady” coefficients underestimate \overline{F}_H .

4.2. Blade-element Analysis Using “steady” Coefficients: Mean Vertical Force

Using data derived from kinematics, we applied a blade-element analysis to calculate forces using two different sets of force coefficients. Lift and drag coefficients from steady-flow measurements of the MAV’s wings applied to the blade-element theory underestimate mean vertical force by a

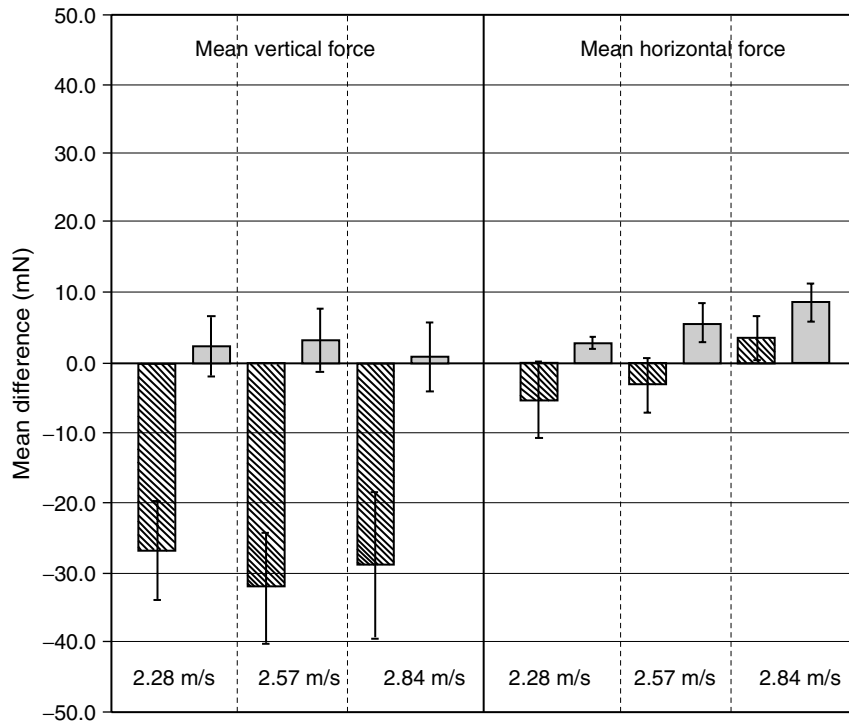


Figure 11: Mean difference (averaged on flapping frequencies, $n = 8$) between mean forces measured with the force balance and mean forces calculated with the blade-element analysis using two sets of force coefficients. Hatched bars = "steady" coefficients, solid bars = "vortex-lift" coefficients. The mean difference can be regarded as an indicator for the offset between experimental measurements and blade-element analyses. In this context, the standard deviation is a measure for the match of the trend of $\overline{F_H}$ (respectively $\overline{F_V}$) vs. flapping frequency. In all cases, the standard deviation of the "vortex-lift" coefficients is considerably lower (between 17% and 84% of the corresponding value from "steady" coefficients) than the standard deviation of the "steady" coefficients.

factor of up to two. Previous studies using a similar method report comparable results: The "quasi-steady" approach has been applied to insects (e.g. [1–3]) and also to slow-speed flapping flight of cockatiels [21], where the wings are exposed to large effective angles of attack. However, in all cases the magnitude of aerodynamic forces observed could not be explained with "quasi-steady" assumptions.

This discrepancy can be related to the effective angle of attack (α_{eff}) during the beat cycle, in particular close to the wing tip (see Figure 12). Our measurements of "steady" coefficients show that $C_{L,max}$ peaks at 11° geometric angle of attack; at higher angles of attack the lift decreases, as the wing stalls in a steady-flow environment. Hence, high flapping frequencies with relatively large α_{eff} will increasingly seriously underestimate C_L . The fact that in the blade-element model the vertical force still increases at increasing α_{eff} is because the wing drag starts to contribute to the vertical force with $\sin(\alpha_{ind}) C_D$ (see Equation 12).

For low flapping frequencies ($f < 5$ Hz), the underestimation of the mean vertical force is less prominent (see Figure 9), because α_{eff} is lower and the lift enhancing effect of leading-edge vortices is less pronounced under these circumstances.

4.3. Blade-element Analysis Using "vortex-lift" Coefficients: Mean Vertical Force

Several studies prove the existence of leading edge vortices in flapping flight and the ability of stably attached vortices to augment lift (e.g. [4, 6, 8, 9, 14]). Stamhuis et al. [16] have shown that LEVs instantly developed on the same type of wing that was flapping with very similar kinematics. An appropriate concept to model C_L and C_D including additional lift created by LEVs was introduced by Polhamus [11]. Using this concept, we model $C_{L,max}$ to be 2.5; a value much higher than $C_{L,max}$ under

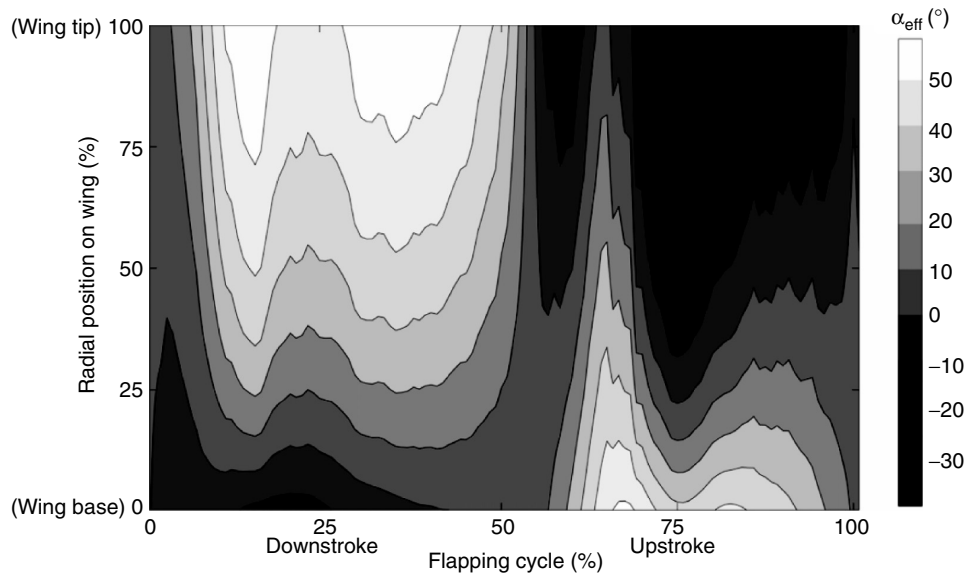


Figure 12: Effective angle of attack as a function of span wise position and flapping cycle. During downstroke and close to the wing tip, the effective angle of attack reaches 50° (see greyscale bar at the right)

steady-flow conditions. Lift coefficients that are much higher than C_L under steady-flow conditions seem to be typical for flapping and pitching airfoils. A numerical study on rapidly pitching airfoils ($Re = 1700$) reveals instantaneous lift coefficients of 2.4 to 3.2 [23]. Similar lift coefficients were reported in a CFD simulation of fruit fly wings ($Re < 1800$), and the presence of a stable LEV is made responsible for increasing C_L up to a value of 3.2 at mid-downstroke of the insect wing [24]. Modelling C_L with a concept that accounts for the additional lift of attached leading-edge vortices hence seems to be a good approximation of aerodynamic phenomena in flapping flight. This is also supported by Dickson and Dickinson [25] who conclude that a “quasi-steady” aerodynamic model may explain the force balance of a hovering insect when appropriate force coefficients are used.

4.4. Blade-element Analysis: Mean Horizontal Force

The blade-element analysis using “vortex-lift” coefficients gives a good estimate of the mean horizontal force ($\overline{F_H}$). The decreasing precision of the match between $\overline{F_H}$ predicted by the blade-element analysis using “vortex-lift” coefficients and experimental data for high flapping frequencies and free flow velocities (see Figure 10B and Figure 11) is not necessarily a limitation of the blade-element model:

In contrast to the balance measurements, which quantify the total drag of the entire MAV system, the blade-element analysis only accounts for the forces created by the wings. The present model does not account for any interference drag generated by the flapping wings. It is very likely, that the tip- and root vortices as well as the accelerated air in the wake of the wings interact with the chassis and the mounting strut during force balance measurements [26]. This situation will increase the total drag of the MAV, and hence decrease the mean horizontal force ($\overline{F_H}$, “thrust”) measured. Our blade-element model does not account for these effects; any result of the analysis using “vortex-lift” coefficients will therefore yield higher values for $\overline{F_H}$ in comparison with the balance measurements (see Figure 10B). An indication of the order of magnitude of interference drag is hard to find in literature as numerous parameters influence interference effects [26]. Tucker [27] proposes a model to quantify the magnitude of interference drag for bird bodies and the mounting struts. The real drag of the bodies was determined to be 10 to 41% lower when taking the interference drag into account. In Tucker’s model, the percentage of interference drag depends amongst other parameters on the ratio of strut drag and measured drag (the latter consists of the drag of the body, the drag of the strut and the interference drag). If the drag of the mounting strut and the drag of the object under test both increase with U_f , the percentage of interference drag will essentially be constant, and its magnitude will increase with the effective flow velocity (influenced by both U_f and flapping frequency). In our study, the increasing difference of $\overline{F_H}$ vs. U_f and flapping frequency of experimental measurements and the “vortex-lift”

blade-element analysis shows a similar increasing trend (see Figure 10B and Figure 11), and might therefore be related to the effect of interference drag. Measuring the interaction of e.g. flapping wings with the chassis and the mounting strut is a challenging task [26], which may be circumvented by a more advanced balance design.

5. CONCLUSION

The aim of this study was to check the feasibility of extending a relatively simple blade-element approach to include additional lift-enhancing aerodynamic effects. A concept initially postulated for sharp-edge delta wings provides data on C_L and C_D under the presence of leading edge vortices. The resulting maximal lift coefficient is a factor of 2.5 greater than typical steady-flow coefficients, and agrees well with data reported in earlier studies on flapping flight. The key requirement for the applicability of the “vortex-lift” approach is the presence of a stable LEV. As Lentink and Dickinson [10] suggest, LEVs in flapping flight are stabilized by the centripetal and Coriolis acceleration. As these accelerations are relatively independent of the Reynolds number [10], it is likely, that the “vortex-lift” approach is not limited to a small bandwidth of flapping wing devices, as long as the advance ratio is low and wing geometry and kinematics create sufficient centripetal and Coriolis accelerations to stabilize the LEV.

We believe that the approach presented in this study might be an appropriate tool to assess and predict forces of flapping-wing flyers and MAVs that operate at low advance ratio and potentially benefit from increased lift enabled by leading edge vortices.

REFERENCES

- [1] Ellington, C. P., The Aerodynamics of Hovering Insect Flight. I. The Quasi-Steady Analysis, *Philosophical Transactions of the Royal Society of London. Series B*, 1984, 305: 1–15
- [2] Ennos, R., The Kinematics and Aerodynamics of the Free Flight of some Diptera, *The Journal of Experimental Biology*, 1989, 142: 49–85
- [3] Zanker J. M. and Gotz K. G., The Wing Beat of *Drosophila melanogaster*. II. Dynamics, *Philosophical Transactions of the Royal Society of London. Series B*, 1990, 327: 19–44
- [4] Ellington, C. P., van den Berg, C., Willmott, A. P. and Thomas, A. L. R., Leading-edge vortices in insect flight, *Nature*, 1996, 384: 626–630
- [5] Usherwood, J. and Ellington, C.P., The aerodynamics of revolving wings. I. Model hawkmoth wings, *The Journal of Experimental Biology*, 2002, 205: 1547–1564
- [6] Bomphrey, R. J., Lawson, N. J., Harding, N. J., Taylor, G. K. and Thomas, A. L. R., The aerodynamics of *Manduca sexta*: digital particle image velocimetry analysis of the leading-edge vortex, *The Journal of Experimental Biology*, 2005, 208: 1079–1094
- [7] Warrick, D. R., Tobalske, B. W. and Powers, D. R., Aerodynamics of the hovering hummingbird, *Nature*, 2005, 435: 1094–1097
- [8] Hubel, T. Y. and Tropea, C., The importance of leading edge vortices under simplified flapping flight conditions at the size scale of birds, *The Journal of Experimental Biology*, 2010, 213: 1930–1939
- [9] Muijres, F. T., Johansson, L. C., Barfield, R., Wolf, M., Spedding, G. R. and Hedenstroem, A., Leading-Edge Vortex Improves Lift in Slow-Flying Bats, *Science*, 2008, 319: 1250–1253
- [10] Lentink, D. and Dickinson, M. H., Rotational accelerations stabilize leading edge vortices on revolving fly wings, *The Journal of Experimental Biology*, 2009, 212: 2705–2719
- [11] Polhamus, E. C., A concept of the vortex lift of sharp-edge delta wings based on a leading-edge-suction analogy, *NASA TN D-3767*, 1966
- [12] Videler, J. J., Stamhuis, E. J. and Povel, G. D. E., Leading-Edge Vortex Lifts Swifts, *Science*, 2004, 306: 1960–1962
- [13] Wu, J., Vakili, A. and Wu, J., Review of the physics of enhancing vortex lift by unsteady excitation, *Progress in Aerospace Sciences*, 1991, Elsevier, 28: 73–131
- [14] Birch J. M. and Dickinson M. H., Spanwise flow and the attachment of the leading-edge vortex on insect wings, *Nature*, 2001, 412: 729–733
- [15] Polhamus, E. C., Application of the leading-edge-suction analogy of vortex lift to the drag due to lift of sharp-edge delta wings, *NASA TN D-4739*, 1968

- [16] Stamhuis, E. J., Thielicke, W., Ros, I. and Videler, J. J., Unsteady aerodynamics essential during low speed flapping flight in bird, submitted for publication, 2011.
- [17] Savile, D. B. O., The Flight Mechanism of Swifts and Hummingbirds, *The Auk*, 1950, 67: 499–504
- [18] Henningson, P., Spedding, G. R. and Hedenstrom, A., Vortex wake and flight kinematics of a swift in cruising flight in a wind tunnel, *The Journal of Experimental Biology*, 2008, 211: 717–730
- [19] Kesel, A. B., Aerodynamic characteristics of dragonfly wing sections compared with technical aerofoils, *The Journal of Experimental Biology*, 2000, 203: 3125–3135
- [20] Kim, D.-K., Han, J.-H., and Kwon, K.-J., Wind tunnel tests for a flapping wing model with a changeable camber using macro-fiber composite actuators, *Smart Materials and Structures*, 2009, 18: 024008
- [21] Hedrick, T., Tobalske, B. and Biewener, A., Estimates of circulation and gait change based on a three-dimensional kinematic analysis of flight in cockatiels (*Nymphicus hollandicus*) and ringed turtle-doves (*Streptopelia risoria*). *The Journal of Experimental Biology*, 2002, 205: 1389–1409
- [22] Kweon, J. and Choi, H., Sectional lift coefficient of a flapping wing in hovering motion, *Physics of Fluids*, 2010, 22: 071703
- [23] Liu, H. and Kawachi, K., A Numerical Study of Insect Flight, *Journal of Computational Physics*, 1998, 146: 124–156
- [24] Wu J. and Sun M., Unsteady aerodynamic forces of a flapping wing, *The Journal of Experimental Biology*, 2004, 207: 1137–1150
- [25] Dickson, W. B. and Dickinson, M. H., The effect of advance ratio on the aerodynamics of revolving wings, *The Journal of Experimental Biology*, 2004, 207: 4269–4281
- [26] Barlow, J. B., Rae, W. H., Jr and Pope, A., *Low-speed Wind Tunnel Testing*, Third edition, Wiley-Interscience, New York, 1999
- [27] Tucker, V. A., Body drag, feather drag and interference drag of the mounting strut in a peregrine falcon, *falco peregrinus*, *The Journal of Experimental Biology*, 1990, 149: 449–468

